Polymer 51 (2010) 1472–1484

Contents lists available at ScienceDirect

Polymer

journal homepage: www.elsevier.com/locate/polymer

Modified interfacial tensions measured in situ in ternary polymer blends demonstrating partial wetting

Nick Virgilio [a], Patrick Desjardins [b], Gilles L'Espérance [c], Basil D. Favis [a,*]

[a] Centre de Recherche En Plasturgie Et Composites (CREPEC), Department of Chemical Engineering, Canada
[b] Regroupement Québécois sur les Matériaux de Pointe (RQMP), Department of Engineering Physics, Canada
[c] Center for Characterization and Microscopy of Materials (CM)^2, École Polytechnique de Montréal, Montréal, Québec H3C 3A7, Canada

ARTICLE INFO

Article history:
Received 21 September 2009
Received in revised form
10 January 2010
Accepted 11 January 2010
Available online 18 January 2010

Keywords:
Ternary polymer blend
Modified interfacial tension
Neumann triangle method

ABSTRACT

An *in situ* Neumann triangle-focused ion beam-atomic force microscopy (NT-FIB-AFM) method has been used to measure modified PS/HDPE interfacial tensions in ternary PS/PP/HDPE blends prepared by melt mixing and demonstrating partial wetting. The ternary blend was modified with SEB, SB and SEBS copolymers. Results related to the position of the PS droplet at the interface show that a symmetrical diblock copolymer is somewhat more efficient in decreasing the interfacial tension compared to an asymmetrical one of similar molecular weight, while the SEBS triblock copolymer appears to have no effect at all. Using the NT-FIB-AFM method, the lowest modified PS/HDPE interfacial tension is 3.0 ± 0.4 mN/m for the symmetric diblock, compared to 4.2 ± 0.6 mN/m ($N = 34$) for the unmodified interface. This corresponds to an apparent areal density in SEB copolymer equal to 0.16 ± 0.03 molecules/nm^2, which is near reported saturation values. By varying the concentration of the copolymer, an emulsification curve reporting the value of the PS/HDPE modified interfacial tension as a function of the apparent areal density of the copolymer at the PS/HDPE interface has been obtained. The interfacial tension values obtained by the NT-FIB-AFM approach are significantly higher than the 0.5 ± 0.2 mN/m ($N = 3$) result obtained by using the classical breaking thread method with the same materials. This discrepancy does not appear to be due to a poor migration of the copolymer to the PS/HDPE interface, but could instead be attributed to the interfacial elasticity of the compatibilized interface, a phenomena that has not been accounted for so far in experimental studies on the morphology of compatibilized multicomponent polymer blends.

1. Introduction

Modifying the interfaces and interfacial tensions in a multiphase polymer blend by the addition of copolymers can result in significant alterations of the morphology, in changes in the relative positions of the phases and in the generation of novel and quite complex types of microstructures [1–6].

Most of the studies that have been performed so far for quantifying the efficacy of copolymers in modifying the interface have been done in the presence of only two homopolymers. The effects of the molecular weight, the architecture and the concentration of copolymers have been particularly investigated. Among the concepts and tools that have been used, the emulsification curve [7–12] and transmission electron microscopy analyses [13–15] have proven to be very reliable and useful. While the emulsification curve provides quantitative information on the efficacy of copolymers at decreasing the phase size and on the apparent areal density of the copolymer at the interface in binary blends, transmission electron microscopy permits to precisely locate the copolymer in the blend and to observe if micelles are formed. However, these two methods do not give any direct information on the value of the modified interfacial tension.

On the other hand, the breaking thread, the pendant drop and the spinning drop methods are frequently used to measure modified interfacial tensions between two immiscible homopolymers [16–22]. For these three techniques, the copolymer must be separately blended with one of the two homopolymers. That system is then placed in contact with the other homopolymer and the interfacial tension experiment is carried out under either static or very low shear conditions. During the experiment, it is expected that the copolymer migrates to the interface and decreases the interfacial tension. Often, disproportionately high copolymer levels

* Corresponding author. Tel.: +1 514 340 4711x4527; fax: +1 514 340 4159.
E-mail address: basil.favis@polymtl.ca (B.D. Favis).

0032-3861/$ – see front matter © 2010 Elsevier Ltd. All rights reserved.
doi:10.1016/j.polymer.2010.01.017

need to be loaded into the particular homopolymer phase in order to ensure that sufficient copolymer migrates to the interface. Furthermore, relatively low molecular weight homopolymers are generally used to maximize the amount of copolymer that can diffuse to the interface during experiment. Although the above interfacial tension techniques do give significant results, the main drawback and challenge has been the copolymer migration issue.

In a typical polymer melt blending operation vigorous melt mixing techniques are known to be quite effective at driving the copolymer to the interface. In binary blends having a matrix/dispersed phase morphology, interfacial tensions calculated with rheological measurements have yielded very interesting results for compatibilized systems [23–29]. Even though the mathematical formalism is relatively heavy and the experimental conditions quite restrictive (the droplets diameter must remain uniform and constant in size during measurements), it is possible to measure a decrease of the interfacial tension as the copolymer is added to the system. However, the addition of a compatibilizer also complicates the analysis due to the copolymer concentration gradients that develop during flow at the interface. Furthermore, multiphase systems remain to be studied using this technique. Clearly, a more simple and in-situ method for measuring the modification of the interfacial tension of polymer blends directly after melt mixing and its effect on the blend microstructure would be the ideal scenario.

Another approach that can provide quantitative data on the interfacial tension in immiscible polymer blends is the Neumann triangle method [30–34]. This equilibrium technique is based on the geometrical analysis of contact between three immiscible phases A, B and C demonstrating partial wetting and a common line of contact (Fig. 1). In that situation, the three spreading coefficients of a ternary immiscible blend are negative [31]. When the effect of the line tension is neglected, the vector sum of the three interfacial tensions acting in the plane perpendicular to the line is equal to zero:

$$\vec{\gamma}_{AB} + \vec{\gamma}_{AC} + \vec{\gamma}_{BC} = \vec{0} \tag{1}$$

The three tensions define three contact angles θ_A, θ_B and θ_C. Using these angles, it is then possible to calculate three interfacial tension ratios Γ_i [30]:

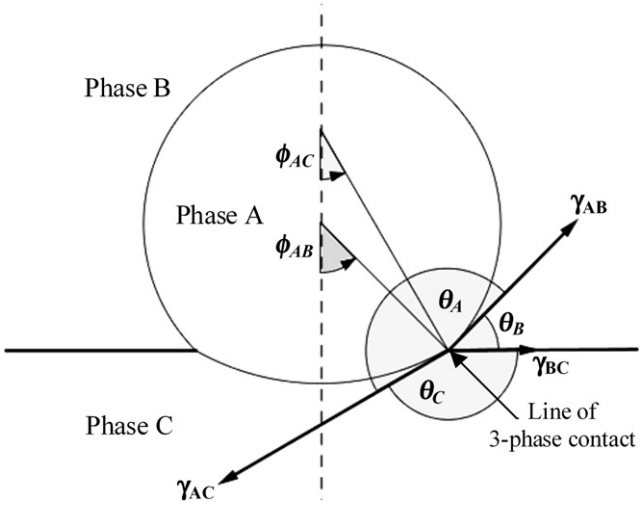

Fig. 1. Geometrical parameters of a ternary blend exhibiting partial wetting [31]. The angles φ_{AB} and φ_{AC} are used to calculate the θ_A, θ_B and θ_C contact angles between the phases at the line of 3-phase contact. γ_{AB}, γ_{AC} and γ_{BC} are the three interfacial tensions.

$$\Gamma_A = \frac{\gamma_{AC}}{\gamma_{AB}} = \frac{\sin\theta_B}{\sin\theta_C} \tag{2a}$$

$$\Gamma_B = \frac{\gamma_{BC}}{\gamma_{AB}} = \frac{\sin\theta_A}{\sin\theta_C} \tag{2b}$$

$$\Gamma_C = \frac{\gamma_{BC}}{\gamma_{AC}} = \frac{\sin\theta_A}{\sin\theta_B} \tag{2c}$$

the Neumann triangle gives relative values of the interfacial tensions. However, it is possible to calculate absolute values when the magnitude of at least one interfacial tension is known.

The use of the Neumann triangle method in multiphase polymer blends has until now been limited to a few cases [35–37], and only for laminate samples prepared under static conditions. One of the main reasons for this is that, until recently, partial wetting morphologies had only been mentioned qualitatively in a limited number of papers [1,37–39] and had not been the subject of a systematic study. In recent work from this laboratory [5,6], we have demonstrated for the first time that partial wetting in multiphase polymer blends prepared by melt mixing can be observed as the dominant morphological state for a wide range of systems. This type of morphology was reported for four different ternary homopolymer blends : 1) polystyrene/polypropylene/high-density polyethylene (PS/PP/HDPE); 2) polystyrene/poly(ε-caprolactone)/polypropylene; 3) poly(L-lactide)/poly(ε-caprolactone)/polystyrene and 4) poly(methyl methacrylate)/polystyrene/polypropylene. In addition, it was shown that the interfacial tension ratios measured directly on the blends *in situ* using the Neumann triangle (NT) method combined with a focused ion beam (FIB) – atomic force microscopy (AFM) morphology preparation technique (NT-FIB-AFM) [6,40] compared well with values obtained using the classical breaking thread method. Furthermore, it was demonstrated that the contact angles could be altered by the addition of an SEB diblock copolymer that selectively modified the PS/HDPE interface. Using this *in situ* Neumann method, a decrease of $\gamma_{PS/HDPE}$ from 4.2 ± 0.6 to 3.3 ± 0.4 mN/m for an apparent areal density of 0.19 ± 0.07 copolymer molecule per nm^2 was measured, while the other two interfaces in that same blend showed no significant interfacial modification. This indicated a selectivity of the SEB for the PS/HDPE interface.

The objective of this work is to examine the potential of the *in situ* NT-FIB-AFM method to measure interfacial tensions in ternary PS/PP/HDPE blends compatibilized with various diblock and triblock copolymers. The compatibilization will be studied as a function of the apparent areal density in copolymer at the interface and the effects of copolymer architecture and copolymer concentration on the PS/HDPE interfacial tension will be investigated.

2. Experimental methods

2.1. Materials

Three homopolymers and five copolymers were used. A barefoot resin of high-density polyethylene, HDPE 3000, was supplied by Petromont. Polypropylene PP PD702 was obtained from Basell and polystyrene PS 615APR from Americas Styrenics. SEB CAP4741 (SEB1), SEB CAP4745 (SEB2) and SEBS G1651 (SEBS), commercial 1,4-hydrogenated styrene-(ethylene-butylene) diblock and 1,4-hydrogenated styrene-(ethylene-butylene)-styrene triblock copolymers, were supplied by Shell. The SEB3 and SB (a styrene-butadiene diblock copolymer) were synthesized at the Center for Education

and Research on Macromolecules (CERM) at the University of Liège, Belgium. The materials characteristics are listed in Table 1.

2.2. Rheology

The rheological characterization of the homopolymers was performed using a SR-5000 controlled stress rheometer from *TA Instruments* in dynamic mode. All experiments were performed using an oscillatory mode in a parallel-plate geometry with a gap of 1.0 mm under a nitrogen atmosphere. The stability of the pure materials was controlled at 1 Hz and 200 °C and a stress sweep was performed to identify the region of linear viscoelasticity. Frequency sweeps were subsequently performed to obtain the zero-shear viscosity of the pure homopolymers, which has been extrapolated by using the modulus of the complex viscosity at low frequencies when the plateau value was reached. In all cases, the loss angles were sufficiently near 90° to consider the homopolymers as non-elastic Newtonian fluids. The rheological properties are reported in Table 1.

2.3. Blend preparation and annealing

All blends contain 10% PS, 45% PP and 45% HDPE, based on volume fractions. The unmodified blend was prepared in a Plasti-Corder Digi-System internal mixer from C W. Brabender Instruments Inc. at 200 °C and 50 RPM for 8 min under a constant nitrogen flow. The blends modified with copolymers were prepared in two steps to maximize the migration of the SEB copolymer at the PS/HDPE interface. Pure PS was initially blended with the required amount of copolymer (grams of copolymer/100 ml of PS) at 180 °C and 50 RPM for 5 min under a constant nitrogen flow and then quenched into cold water. The modified ternary blends were prepared subsequently with the required amount of PS + copolymer, at 200 °C and 50 RPM for 8 min of mixing under a constant nitrogen flow. A small amount (0.2% wt.) of Irganox B-225 from Ciba–Geigy was added to all blends in order to prevent thermal degradation. After blending, the materials were quenched in cold water to freeze-in the morphology. Quiescent annealing was then performed at 200 °C for 30 min and the samples were finally plunged into cold water to freeze-in the morphology.

2.4. Breaking thread for interfacial tension measurement

All unmodified interfacial tensions were measured using the breaking thread method [41,42]. For the $\gamma_{PS/HDPE}$ and $\gamma_{PS/PP}$ interfacial tensions, PS threads with diameters ranging from 30 to 60 μm were first annealed at 100 °C under vacuum to remove the residual stress. They were subsequently sandwiched between HDPE or PP films, respectively. For the $\gamma_{PP/HDPE}$ interfacial tension measurement, PP threads were sandwiched between HDPE films.

Table 2
Interfacial tensions by the breaking thread method and resulting spreading coefficients.

Polymer pairs	Interfacial tensions γ (mN/m)	Spreading coefficients λ (mN/m)	
HDPE/PS	4.9 ± 0.6 (N = 5)	$\lambda_{HDPE/PS/PP}$	−6.5 ± 1.3
PP/PS	3.5 ± 0.2 (N = 4)	$\lambda_{HDPE/PP/PS}$	−0.5 ± 1.3
HDPE/PP	1.9 ± 0.5 (N = 2)	$\lambda_{PP/HDPE/PS}$	−3.3 ± 1.3
HDPE/PS modified with 20% SEB3	0.5 ± 0.2 (N = 3)		

A PS/HDPE modified interfacial tension was also measured using the breaking thread method in order to compare with the Neumann triangle results. The HDPE was initially blended with 20% wt. of SEB3 at 200 °C for 5 min at 50 RPM. The PS threads were then sandwiched between two (HDPE + copolymer) films and the laminates were annealed during 24 h at 130 °C under vacuum. Measurements were then performed at 200 °C using an Optiphot-2 microscope from Nikon and a Mettler FP-82HT hot-stage connected to a Mettler FP-90 central processor. Digital images were captured and analyzed using Streampix v.III and Visilog v.6.3 software applications, provided by Norpix. Five measurements were performed for each tension, except for the $\gamma_{PP/HDPE}$ tension for which only two were obtained. The polymers were initially blended with Irganox B-225 (0.2% wt.) to prevent thermal degradation during the experiment. The interfacial tension values and the spreading coefficients for the PS/PP/HDPE blend are reported in Table 2. In comparison, Guo et al.[2] reported values of 5.9, 5.1 and 1.1 mN/m respectively for the HDPE/PS, PP/PS and HDPE/PP interfacial tensions, which follow similar trends to ours.

2.5. Scanning electron microscope observations

Samples were initially cryogenically microtomed using a Leica RM2165 microtome equipped with a LN21 cooling system. For SEM observations, the PS phase was subsequently extracted at room temperature for three days using cyclohexane as a selective solvent and then dried for 2 days at 60 °C under vacuum in an oven. The samples were then coated with a gold-palladium layer by plasma sputtering. SEM observations were conducted using a JEOL JSM 840 scanning electron microscope operated at 10 kV and $6x10^{-11}$ A.

2.6. Focused ion beam sample preparation and atomic force microscopy analysis

Samples for the focused ion beam (FIB) preparation were first cryogenically microtomed. A gold-palladium layer was then deposited on the samples by plasma sputtering and the surface of the specimens was subsequently etched with a focused ion beam. FIB surface milling was performed using a Hitachi 2000A Ga^+

Table 1
Materials characteristics.

Polymers	$M_n \times 10^{-3}$(g/mol)[a]	% Styrene	Melt Index (g/10 min)[a]	$\eta^* \times 10^{-3}$ (Pa.s)[b] at 200 °C and 25s^{-1}	$\eta_0 \times 10^{-3}$ (Pa.s)[c] at 200 °C
HDPE	–	–	8	0.42	1.1
PP	89	–	35	0.27	0.71
PS	95 (M_w)	–	14	0.49	4.04
SEB1	67	30	–	–	–
SEB2	187	26	–	–	–
SEB3	63	53	–	–	–
SB	450	39	–	–	–
SEBS	174	33	–	–	–

[a] Obtained from suppliers.
[b] Modulus of the complex viscosity at a frequency of 25 s^{-1}.
[c] Zero-shear viscosity.

Table 3
Average values and standard deviations of the geometrical parameters of the PS droplets – effect of the copolymer architecture.

Blend	# Samples (N)	θ_{PS}°	θ_{PP} °	θ_{HDPE} °	$r_{PS/PP}$ (μm)	$r_{PS/HDPE}$ (μm)
Unmodified	34	170 ± 5	49 ± 11	141 ± 8	2.4 ± 1.4	2.8 ± 1.6
1% SEB1	39	165 ± 9	107 ± 10	88 ± 12	3.6 ± 0.9	3.5 ± 0.9
1% SEB3	26	165 ± 7	124 ± 18	71 ± 22	4.3 ± 0.3	3.8 ± 0.3

Table 5
Average values and standard deviations of the geometrical parameters of the PS droplets – effect of the SEB3 copolymer concentration

Blend	# samples (N)	θ_{PS}°	θ_{PP}°	θ_{HDPE}°	$r_{PS/HDPE}$ (μm)	$r_{PS/HDPE}$ (μm)
Unmodified	34	170 ± 5	49 ± 11	141 ± 8	2.4 ± 1.4	2.8 ± 1.6
0.1%	20	167 ± 4	54 ± 9	139 ± 7	3.5 ± 0.6	4.1 ± 0.7
0.5%	24	165 ± 8	97 ± 22	98 ± 19	4.4 ± 0.9	4.4 ± 0.9
1%	26	165 ± 7	124 ± 18	71 ± 22	4.3 ± 0.3	3.8 ± 0.3

focused ion beam operated at 30 keV and 3 nA, with an etching window of 120 x 10 μm^2 and a dwelling time of 3 μsec. The etched surface was then analyzed by AFM in tapping mode using a Dimension 3100 scanning probe microscope from Veeco Instruments equipped with a Nanoscope IVa control module. Tips model PPP-NCH-W from Nanosensors, with a resonance frequency of 204–497 kHz, a force constant of 10–130 N/m, length and width of 125 ± 10 μm and 30 ± 7.5 μm, and tip height of 10–15 μm and radius < 10 nm were used. Topographic (height) images were subsequently treated with the AFM software to remove the effects caused by the inclination of the samples and curtain effect produced by FIB surface preparation. Details concerning the procedure are given in a previous paper [40].

2.7. The Neumann triangle method for interfacial tension analysis

The Neumann triangle method was conducted on the AFM images of the samples treated initially with the FIB. As shown in Fig. 1, the PS phase was designated as phase A, PP as phase B and HDPE as phase C. The contact angles are thus $\theta_A = \theta_{PS}$, $\theta_B = \theta_{PP}$ and $\theta_C = \theta_{HDPE}$ and the interfacial tension ratios are given by $\Gamma_A = \Gamma_{PS}$, $\Gamma_B = \Gamma_{PP}$ and $\Gamma_C = \Gamma_{HDPE}$. The absolute interfacial tensions are $\gamma_{AB} = \gamma_{PS/PP}$, $\gamma_{AC} = \gamma_{PS/HDPE}$ and $\gamma_{BC} = \gamma_{PP/HDPE}$. In our case, since phase C (HDPE) is also a major phase, note that $\phi_{PP/HDPE}$ (ϕ_{BC}) tends to zero and $r_{PP/HDPE}$ (r_{BC}) tends to infinity.

For the procedure, the PS/PP and PS/HDPE interfaces are first completed to full circles, and their centers are joined by a common segment defining a symmetrical axis of rotation. Following this, the center of each circle is joined to the line of 3-phase contact by the radius of curvature $r_{PS/PP}$ (r_{AB}) and $r_{PS/HDPE}$ (r_{AC}). The angles $\phi_{PS/PP}$ (ϕ_{AB}) and $\phi_{PS/HDPE}$ (ϕ_{AC}) are comprised by the axis of symmetry of the system and the radius of curvature joining the circles' origins to the 3-phase line of contact. The contact angles are calculated using the following equations [31]:

$$\theta_{PS} = \phi_{PS/HDPE} + \pi - \phi_{PS/PP} \quad (3a)$$

$$\theta_{PP} = \phi_{PS/PP} \quad (3b)$$

$$\theta_{HDPE} = \pi - \phi_{PS/HDPE} \quad (3c)$$

This approach was used because of the uncertainty associated with directly tracing tangent lines at the 3-phase line of contact. Finally, knowing the θ_i angles, the relative interfacial tensions Γ_i were calculated using equations 2a-c. The average values and associated standard deviations are reported in Tables 3 to 6, with the number of measurements N (equal to the number of analyzed particles multiplied by two) performed for each blend.

The experimental errors on the reported interfacial tension ratios were analyzed in a previous work [6]. The major source of error appears to come from the non-perpendicular intersection of the 3-phase line with the cutting plane. A numerical simulation done with a similar system suggests that in order to minimize this source of error, only the largest analyzed particles should be considered. This approach indicates that the difference between the measured apparent interfacial tension ratios and the true values varies between 5 and 15%, which is an acceptable difference as compared to other methods. Finally, the experimentally measured standard deviations compare well with the ones obtained by simulation.

More details concerning the geometrical analysis and the general analysis of the method can be found elsewhere [6,31].

3. Results and discussion

3.1. PS droplet position at the PP/HDPE interface

Fig. 2 shows the morphology of the unmodified (Fig. 2a) and modified PS/PP/HDPE blends after a 30 min annealing treatment. As reported in previous works [5,6], it clearly appears that the unmodified PS droplets have an affinity for the PP/HDPE interface, as predicted by the three negative spreading coefficients (Table 2). The PS droplets preferentially locate on the PP side of the PP/HDPE interface since $\gamma_{PS/PP}$ is lower than $\gamma_{PS/HDPE}$. However, a significant fraction of the PS droplets reside inside the PP phase, while their segregation from the HDPE phase is complete. Note that similar trends were observed when using a PP of higher viscosity, a PS of lower molecular weight, or with an increase in the time of mixing [5].

The addition of a small amount of copolymer significantly modifies the morphology (Fig. 2b–f). The effect of 1% SEB1 (Fig. 2b) has been studied previously [5,6]. The PS droplets are located exclusively at the PP/HDPE interface and form a very dense array after a short period of quiescent annealing time, accompanied by a suppression of coalescence. Furthermore, they are approximately located symmetrically at the PP/HDPE interface. Assuming that the SEB1 copolymer preferentially locates at the PS/HDPE interface and decreases the corresponding interfacial tension, a reasonable hypothesis since the PS droplets migrate towards the HDPE phase, this morphology modification can be explained by using the spreading coefficients (Fig. 3) [4]:

Table 4
Average values and standard deviations of the interfacial tension ratios - effect of the copolymer architecture.

Blend	Γ_{PS}	Γ_{PP}	Γ_{HDPE}	$\gamma^{mod}_{HDPE/PS}$ (mN/m)	$\Delta\gamma_{HDPE/PS}$ (mN/m)	Σ_{app} (copolymer molecules/nm^2)
Unmodified	1.2 ± 0.1	0.3 ± 0.15	0.2 ± 0.1	4.2 ± 0.6	–	–
1% SEB1	0.95 ± 0.05	0.3 ± 0.15	0.3 ± 0.15	3.3 ± 0.4	0.9 ± 0.6	0.20 ± 0.07
1% SEB3	0.87 ± 0.07	0.3 ± 0.1	0.3 ± 0.1	3.0 ± 0.4	1.2 ± 0.7	0.16 ± 0.03

Table 6
Effect of the copolymer concentration on the relative interfacial tensions

%SEB3 in blend	Γ_{PS}	Γ_{PP}	Γ_{HDPE}	$\gamma^{mod}_{HDPE/PS}$ (mN/m)	$\Delta\gamma_{HDPE/PS}$ (mN/m)	Σ_{app} (copolymer molecules/nm^2)
Unmodified	1.2 ± 0.1	0.3 ± 0.15	0.2 ± 0.1	4.2 ± 0.6	–	–
0.1%	1.2 ± 0.1	0.3 ± 0.1	0.3 ± 0.1	4.2 ± 0.6	0.0 ± 0.2	0.07 ± 0.03
0.5%	0.99 ± 0.03	0.3 ± 0.1	0.3 ± 0.1	3.5 ± 0.3	0.75 ± 0.5	0.12 ± 0.02
1%	0.87 ± 0.07	0.3 ± 0.1	0.3 ± 0.1	3.0 ± 0.4	1.2 ± 0.7	0.16 ± 0.03

$$\lambda_{PP/PS/HDPE} = \gamma_{HDPE/PP} - \left(\gamma_{HDPE/PS} + \gamma_{PP/PS}\right) \quad (4a)$$

$$\lambda_{PP/PS/HDPE} = \gamma_{HDPE/PS} - \left(\gamma_{HDPE/PP} + \gamma_{PP/PS}\right) \quad (4b)$$

$$\lambda_{PS/HDPE/PP} = \gamma_{PP/PS} - \left(\gamma_{HDPE/PP} + \gamma_{HDPE/PS}\right) \quad (4c)$$

When no interfacial modifier is added, all three spreading coefficients are negative, with $\lambda_{PS/HDPE/PP}$ being smaller than $\lambda_{PS/PP/HDPE}$. This would predict PS droplets should preferentially lie on the PP side of the PP/HDPE interface (Fig. 3a). However, $\gamma_{PS/HDPE}$ decreases by adding the SEB1 copolymer. When the modified PS/HDPE interfacial tension ($\gamma^{mod}_{PS/HDPE}$) decreases and becomes equal to $\gamma_{PS/PP}$ (3.5 mN/m, Table 2), the droplets are then predicted to be half in the HDPE phase and half in the PP phase, as the schematic of Fig. 3b shows. When $\gamma^{mod}_{PS/HDPE}$ decreases below $\gamma_{PS/PP}$, $\lambda_{PS/HDPE/PP}$ becomes larger than $\lambda_{PS/PP/HDPE}$ and the PS droplets will preferentially relocate on the HDPE side of the PP/HDPE interface (Fig. 3c). Finally, if $\gamma^{mod}_{PS/HDPE}$ decreases below 1.6 mN/m, the PS droplets are predicted to relocate exclusively into the HDPE phase (Fig. 3d).

The influence of a number of copolymer interfacial modifiers (SEB1, SEB2, SEB3, SB and SEBS) is examined in Fig. 2b–f. In almost all cases (except for the SEBS), the addition of the copolymer significantly increases the fraction of PS droplets located at the PP/HDPE interface and decreases the fraction located in the PP phase. This indicates a significant interfacial activity of the copolymer

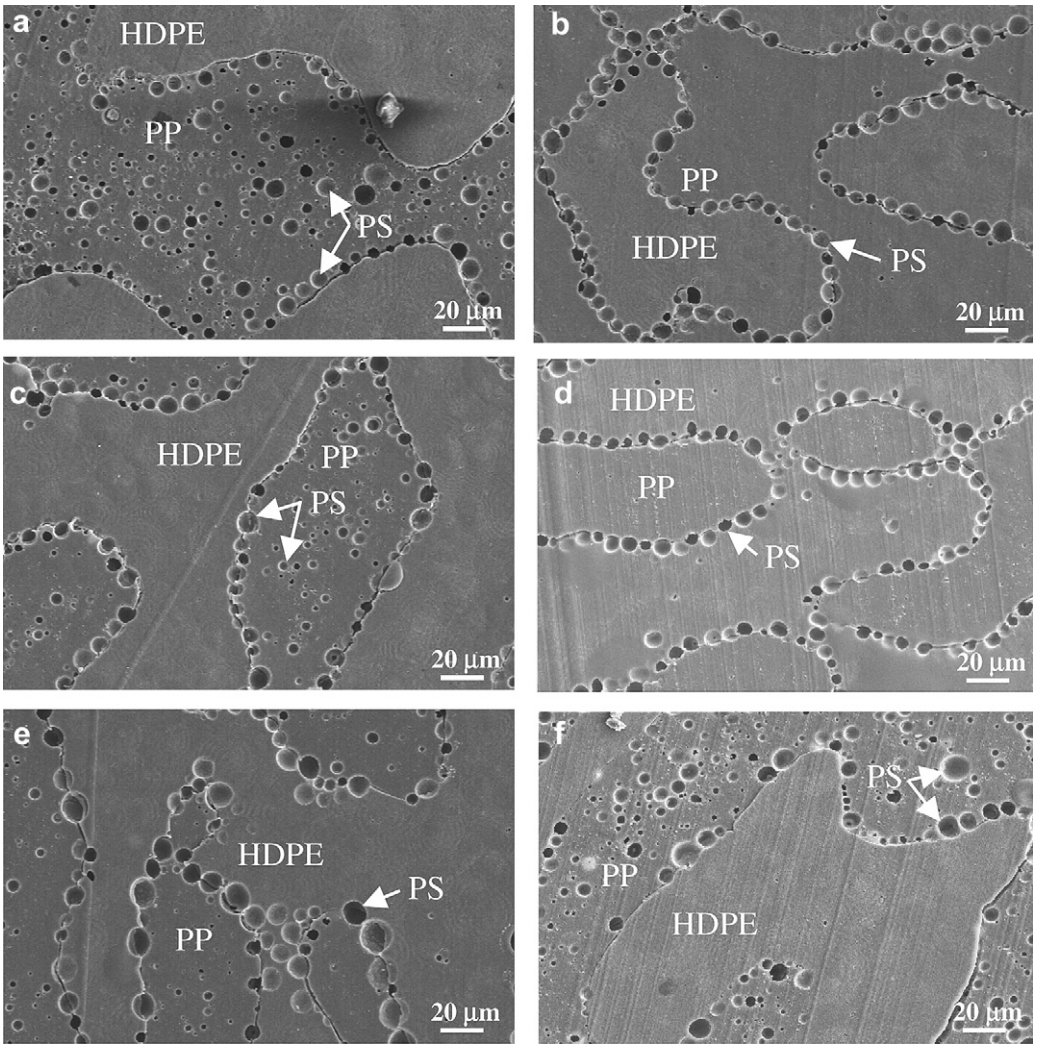

Fig. 2. Effect of the copolymer architecture on the morphology of PS/PP/HDPE 10/45/45 blends. a) Unmodified blend; b) 1% SEB1 (based on PS content); c) 1% SEB2; d) 1% SEB3; e) 1% SB; f) 1% SEBS. Note that the PS has been selectively extracted to increase the contrast between the phases. In b) and d) all PS particles are located at the PE/PP interface.

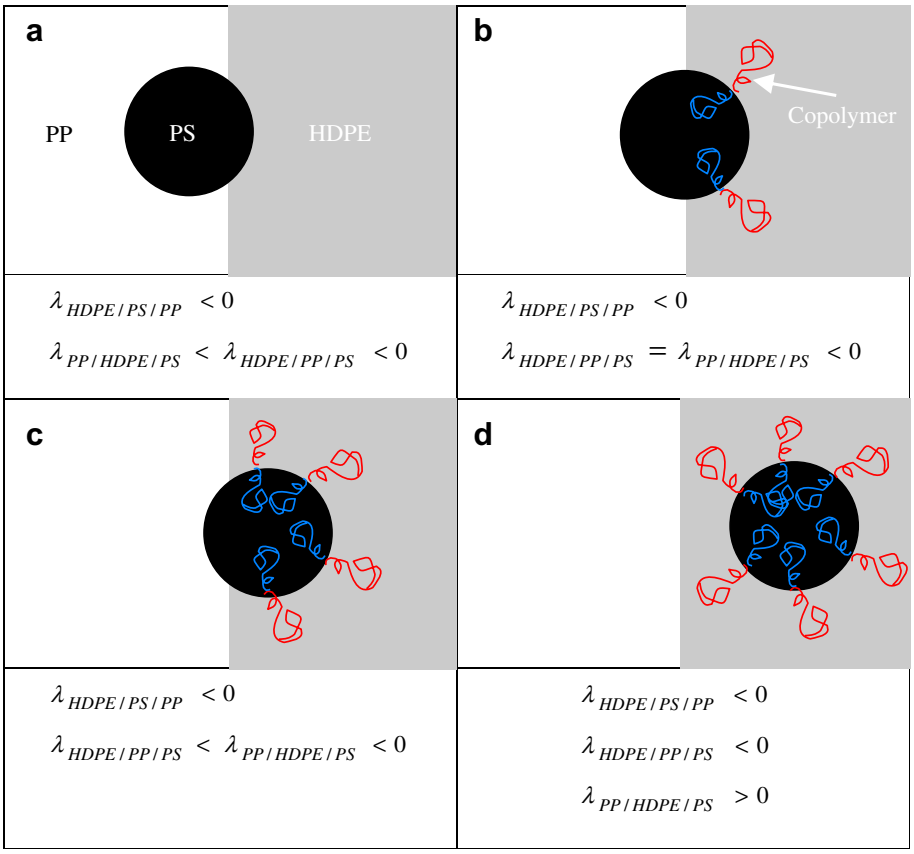

Fig. 3. Effect on the morphology for a copolymer having an affinity for the PS/HDPE interface in a PS/PP/HDPE 10/45/45 blend. a) Initial morphology, when no compatibilizer is added; b) $\gamma^{mod}_{PS/HDPE}$ modified with a copolymer is equal to $\gamma_{PP/PS}$ (3.5 mN/m), and the PS droplets are symmetric at the HDPE/PP interface; c) 1.6 mN/m $< \gamma^{mod}_{PS/HDPE}$ modified with copolymer $<$ 3.5 mN/m. The PS droplets are on the HDPE side of the HDPE/PP interface and d) $\gamma^{mod}_{HDPE/PS}$ modified with copolymer $<$ 1.6 mN/m, PS droplets are in the HDPE phase.

even at a low concentration of 1%. All copolymers, except the SEBS (Fig. 2f), seem to have a significant affinity for the PS/HDPE interface, resulting in a decrease of $\gamma_{PS/HDPE}$ and a migration of the PS droplets towards the HDPE phase. Although the relative efficacies of the SEB3 (Fig. 2d) and SEB1 (Fig. 2b) copolymers look similar, the PS droplets are generally located more on the HDPE side for the SEB3 case. This is more apparent when comparing Fig. 4a (SEB1) and 4b (SEB3). It is also very clear that the triblock copolymer appears to have a negligible effect on the resulting morphology (Fig. 2f). These results show that the best performance on reducing the PS/HDPE interfacial tension, as derived from the relative position of the PS droplets at the PP/HDPE interface, is for the symmetrical diblock SEB3 (63 K mol. wt.); then SEB1 (67 K), an asymmetrical diblock; SB (450 K) and SEB2 (187 K) perform less well and SEBS (174 K) has virtually no effect on driving PS droplets to the interface.

These data indicate that three factors influence the results: composition of the copolymer (symmetric is better than asymmetric); the architecture of the copolymer (diblock is better than triblock); and the molecular weight (low molecular weight modifiers are more effective). We can thus qualitatively classify the efficacy of the different copolymers by their ability to drive PS droplets to the interface and by their effect on relocating the PS droplets from the PP side of the PP/HDPE interface to the HDPE side and into the HDPE phase in order of decreasing efficacy:

SEB3 > SEB1 > SB ≈ SEB2 > SEBS

It is important to underline that the process described above for the compatibilization of partially wet systems is quite different from that of the classic compatibilization of a binary blend. In classic compatibilization the modifier must simply find its way, through the phase in which it was added, to the interface. In this partial wetting system, the volume restriction of the interfacial modifier is more severe. In this latter case, the PS droplet containing the modifier must find its way to the PP/HDPE interface and once there, the modifier in turn needs to saturate and concentrate at the PS/HDPE interface. In previous work on the same materials systems [5], it was shown that the melt mixing of partial wetting PS/PP/HDPE systems containing SEB1 block copolymer is quite effective at driving the PS droplet to the interface. However, the first several minutes of annealing after mixing (for SEB1) were necessary to complete the concentration and saturation of the copolymer at the interface as evidenced by the total suppression of coalescence during annealing after 30 min. It is entirely likely that the migration effects related to the saturation of the interface during annealing tend to exaggerate effects such as molecular weight and architecture in these partially wet systems and hence a poorer performance is observed for the SB, SEB2 and SEBS copolymers. Nevertheless, the extremely poor performance of the triblock at even driving the PS droplets to the interface is surprising and will require further work to understand fully. For the best performing modifiers (SEB3 and SEB1), a somewhat better performance is observed for SEB3 (symmetric composition) as compared to SEB1 (asymmetric composition). Leibler [43,44] has shown that diblock copolymers of symmetrical composition should be more effective at reducing the interfacial tension than an asymmetrical one.

For all cases in the above study, it appears clear that the modified interfacial tension does not decrease below 1.6 mN/m, since

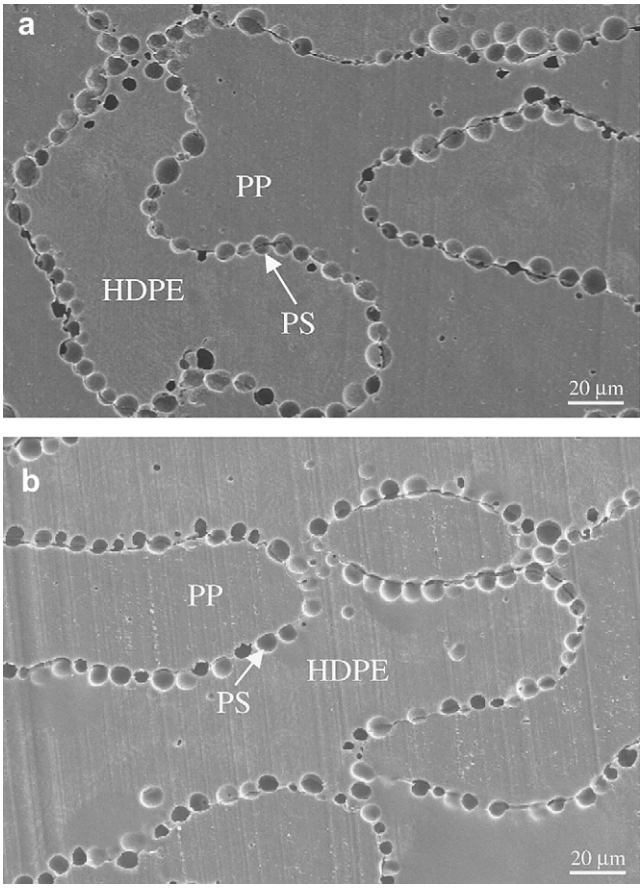

Fig. 4. SEM micrographs of annealed PS/PP/HDPE 10/45/45 blends modified with a) 1% SEB1 and b) 1% SEB3. The PS droplets are more on the HDPE side of the PP/HDPE interface for 1% SEB3. Note that the PS has been extracted to increase the contrast between the phases.

complete segregation of the PS droplets inside the HDPE phase is not observed [4]. In the next section the modified interfacial tension will be studied by using an *in situ* Neumann triangle method [5].

3.2. Measuring the interfacial tension of modified systems using the Neumann triangle method

Using an *in situ* Neumann triangle method combined with FIB-AFM sample preparation and analysis [6,40], we have measured the interfacial tension ratios directly in PS/PP/HDPE 10/45/45 (%vol.) blends containing 0% copolymer, 1% SEB1 or 1% SEB3 after 30 min of quiescent annealing time. The FIB-AFM image of Fig. 5a shows the morphology of the uncompatibilized case, while Fig. 5b and c show the 1% SEB1 and 1% SEB3 blends, respectively. Fig. 6 shows examples of the geometric constructions used to measure the interfacial tension ratios [6]. The results are reported in Tables 3 and 4.

$\Gamma_{PP}(\gamma_{PP/HDPE}/\gamma_{PS/PP})$ shows no significant modification when the compatibilizers are added, indicating that both the $\gamma_{PP/HDPE}$ and $\gamma_{PS/PP}$ interfacial tensions are most probably not significantly modified by the copolymers [6]. However, Γ_{PS} decreases significantly when the copolymers are added. From $\Gamma_{PS} = 1.2 \pm 0.1$ ($N = 34$) with no compatibilizer, it decreases to 0.95 ± 0.05 ($N = 39$) and 0.87 ± 0.07 ($N = 26$) after the addition of 1% SEB1 and 1% SEB3, respectively. Using the value of $\gamma_{PS/PP} = 3.5 \pm 0.2$ mN/m ($N = 4$) (Table 2) with Γ_{PS}, the PS/HDPE interfacial tension decreases from 4.2 ± 0.6 mN/m ($N = 34$) to 3.3 ± 0.4 mN/m ($N = 39$) and 3.0 ± 0.4 mN/m ($N = 26$) for the SEB1 and SEB3 copolymers. These results point to respective interfacial tension drops of 0.9 ± 0.6 and 1.2 ± 0.7 mN/m.

It is possible to calculate the apparent areal density Σ_{app} of the copolymer at the modified interface if it is assumed that the copolymer is initially homogeneously distributed in the PS phase and that it subsequently relocates completely at the PS/HDPE interface. This assumption is justified based on a number of observations for SEB1 and SEB3. Firstly, previous work on SEB1 showed that after 30 min of annealing, this copolymer was able to completely suppress any further coalescence of the system. This is a strong support that the copolymer is highly localized at the interface since the coalescence of the unmodified system was significant even after 120 min of quiescent annealing time. More support is given by Figs. 7 and 8, which show the morphology of the system as the amount of copolymer gradually increases, after 30 min of quiescent annealing time. In addition to the migration of the PS droplets towards the HDPE phase, it can be seen that there is a clustering of the PS droplets at the PP/HDPE interface and a formation of a close-packed structure, indicating an inhibition of coalescence due to steric repulsions between neighbouring SEB3 covered PS droplets. Furthermore, FIB/AFM analysis of the PS phase showed no indication of any copolymer micelle formation. The apparent areal density Σ_{app} of the copolymer can then be calculated geometrically by dividing the amount of copolymer within the droplet (whose volume can be divided in two parts, one within the PP phase and one within the HDPE) by the PS/HDPE interfacial area [5,6,8–15,31]:

$$\text{Vol. of PS in PP} : \frac{\pi}{3} r_{PS/PP}^3 \left(2 + 3\cos\left(\phi_{PS/PP}\right) - \cos^3\left(\phi_{PS/PP}\right)\right)$$

$$\text{Vol. of PS in PE} : \frac{\pi}{3} r_{PS/HDPE}^3 \left(2 - 3\cos\left(\phi_{PS/HDPE}\right) + \cos^3\left(\phi_{PS/HDPE}\right)\right)$$

$$\text{Area of PS/HDPE interface} : 2\pi r_{PS/HDPE}^2 \left(1 - \cos\phi_{PS/HDPE}\right)$$

$$\Sigma_{app} = \frac{\text{Total volume of PS droplet}}{\text{Area of PS/HDPE interface}} \times \frac{\phi_{copo} N_{Av}}{M_w} \quad (5)$$

where ϕ_{copo} is the concentration of the block copolymer in g/100 ml of PS, N_{av} is Avogadro's number and M_w is the molecular weight of the copolymer. For the 1% SEB1 blend, the average apparent areal density is 0.20 ± 0.06 copolymer molecule/nm^2, while it is 0.16 ± 0.03 copolymer molecules/nm^2 for the 1% SEB3 blend. SEB3 appears to be a better compatibilizer, which could be due to its symmetry. Similar areal density values between 0.1 and 0.2 copolymer molecules/nm^2 are reported in the literature for saturated interfaces of such copolymers [10,11,14,15].

Figs. 7 and 8 show the morphology of the PS/PP/HDPE 10/45/45 blends after 30 min of quiescent annealing when the concentration in SEB3 is gradually increased from 0% to 2% based on the PS content. There is a gradual re-localization of the PS droplets from the PP side of the PP/HDPE interface to the HDPE side as the concentration in SEB3 increases. At 0.1% SEB3, the effect is almost imperceptible (Figs. 7b and 8a). At 0.5% SEB3, there is already a significant re-localization of the PS droplets on the HDPE side of the PP/HDPE interface, as the micrograph of Fig. 7c and the FIB-AFM image of Fig. 8b show. At 1% and 2% SEB3, the transfer is clear and a decrease in PS droplet size is observed (Fig. 7d–e and 8c-d).

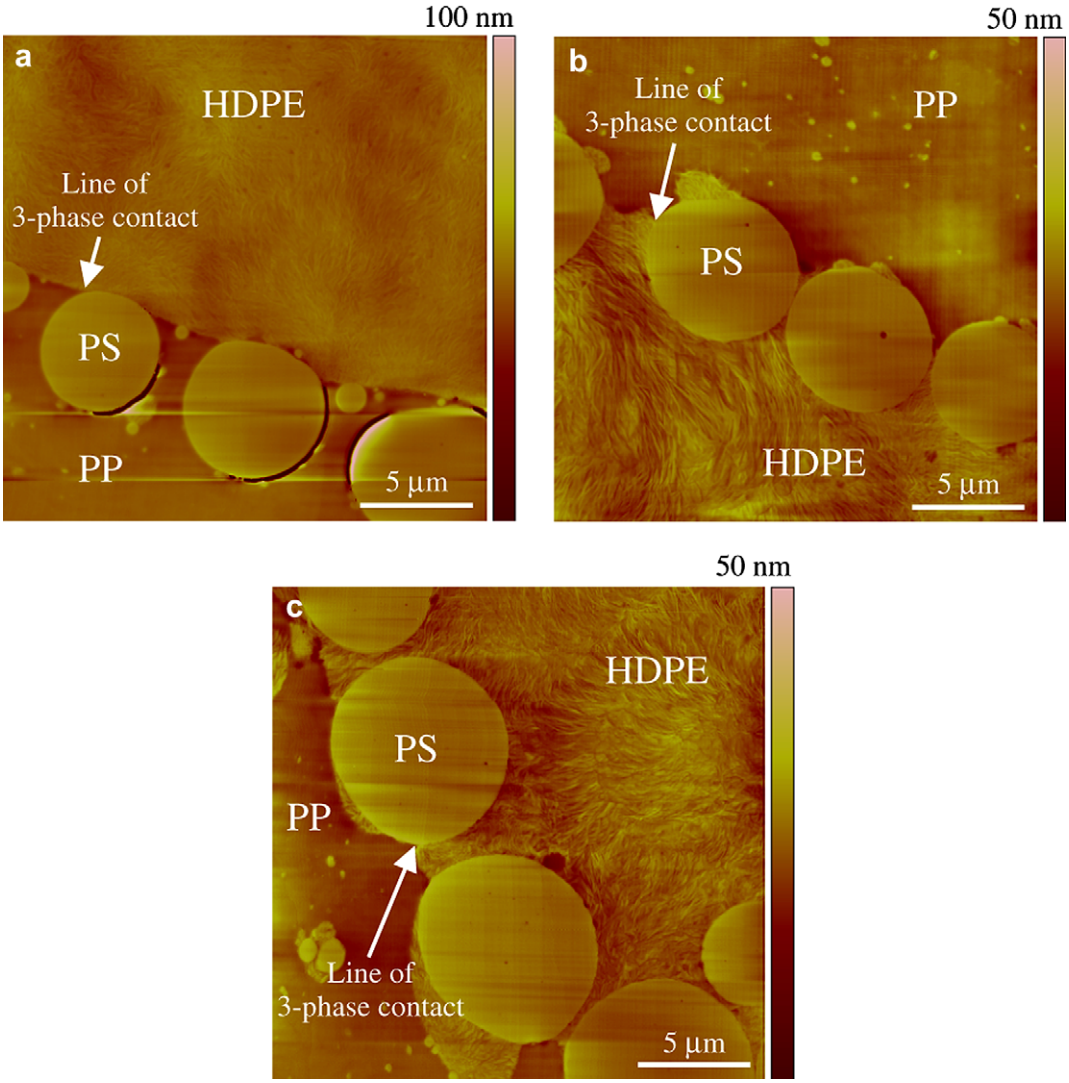

Fig. 5. FIB-AFM images of PS/PP/HDPE 10/45/45 %vol. blends after 30 min of quiescent annealing used for the Neumann triangle analysis with a) 0% copolymer; b) 1% SEB1 and c) 1% SEB3.

Furthermore, at 2% SEB3, PS droplets start to form clusters, indicating a partial or complete suppression of coalescence, as reported previously [5].

The contact angles and interfacial tension ratios are reported in Tables 5 and 6. At 0.1% SEB3 (Fig. 8a), the effect is not perceptible since Γ_{PS} (0.1% SEB3) = Γ_{PS} (uncompatibilized) = 1.2 ± 0.1 ($N = 20$). At 0.5% SEB3 (Fig. 8b), $\Gamma_{PS} = 0.99 \pm 0.03$ ($N = 24$) and it decreases to a value of 0.87 ± 0.07 ($N = 26$) at 1% SEB3 (Fig. 8c). Using the value $\gamma_{PS/PP} = 3.5 \pm 0.2$ mN/m ($N = 4$) and the Γ_{PS} values in Table 6, $\gamma_{PS/HDPE}$ decreases from 4.2 ± 0.6 mN/m ($N = 34$) to 3.5 ± 0.3 mN/m ($N = 24$) and 3.0 ± 0.4 mN/m ($N = 26$) when 0.5% and 1% SEB3 are added.

The apparent areal densities are: 0.07 ± 0.03 copolymer molecule/nm^2 for the 0.1% SEB3 blend; 0.12 ± 0.02 copolymer molecule/nm^2 for the 0.5% SEB3 blend and 0.16 ± 0.03 copolymer molecule/nm^2 for the 1% SEB3 blend. Measurements with the 2% SEB3 blends were not considered reliable due to the close contact and deformation of the PS droplets (see Fig. 8d). However, it is clear that the apparent modified interfacial tension does not decrease below 1.6 mN/m which is the limiting interfacial tension for partial wetting [4].

Fig. 9 shows the value of $\gamma^{mod}_{PS/HDPE}$ as a function of the apparent areal density of the SEB3 at the PS/HDPE interface. The standard deviations σ and the 95% confidence intervals (CI) ($= 1.96\sigma/\sqrt{N}$) are given, the latter indicating the uncertainties on the average interfacial tensions and apparent areal densities. This is the first experimental study showing the dependence of interfacial tension on areal density of copolymer at the interface. It is interesting to note that the dependence of the decrease in interfacial tension shown here in Fig. 9 compares well with that theoretically predicted from simulation studies in another work [45].

3.3. Comparison of the results with the breaking thread method

A significant discrepancy is observed between the magnitude of the interfacial tension values shown in Fig. 9 for the modified interfaces in this study and other reported values in the literature. Most of those other results have been obtained using the classical breaking thread method. Mekhilef et al. [19] reported a decrease from 5.6 mN/m to 1.1 mN/m for a PS/HDPE blend with an SEBS triblock copolymer. Elemans et al. [21] reported a decrease from 4.7 to 1.1 mN/m for a PE/PS blend compatibilized with a diblock SEB

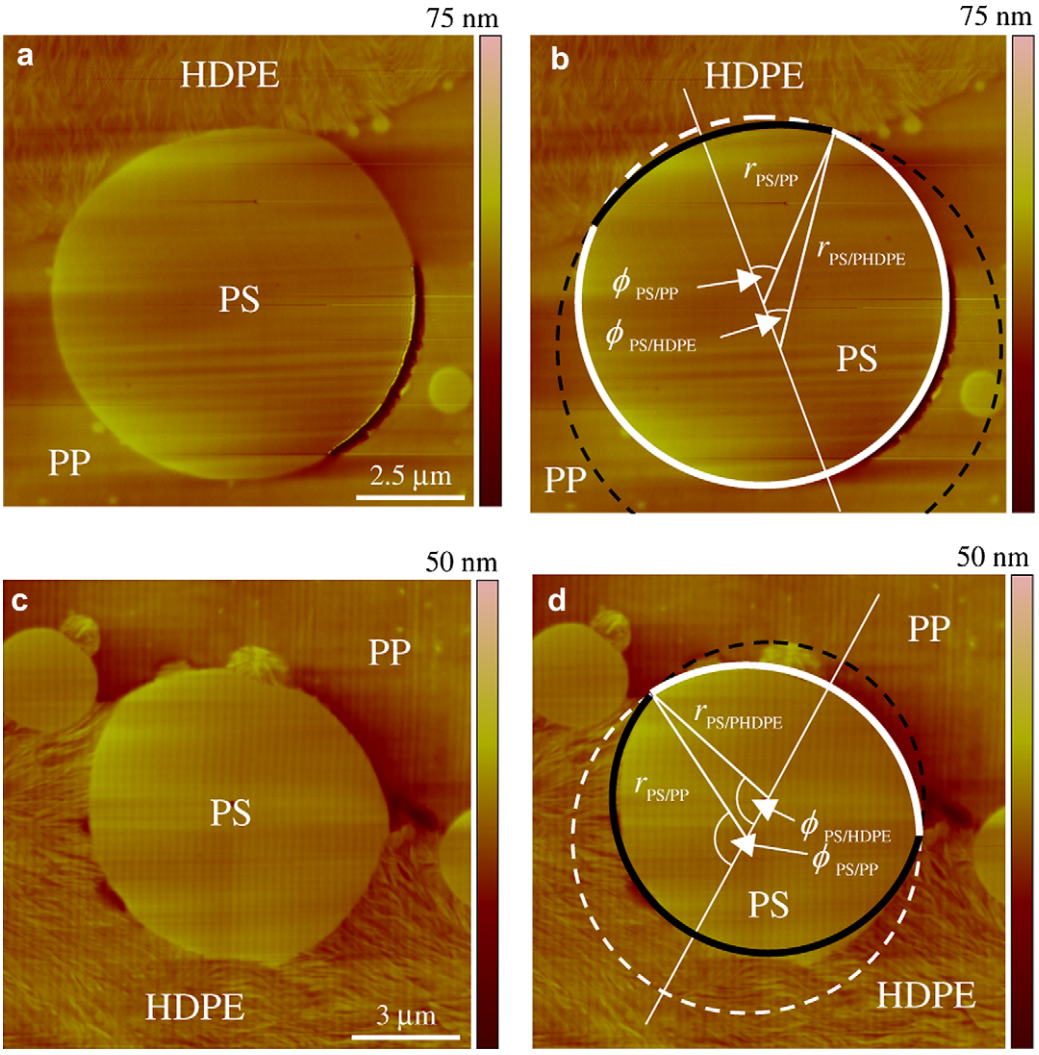

Fig. 6. Geometrical construction displaying the fitted circles and the ϕ angles used to calculate the contact angles θ, and the radius of curvature of the PS/HDPE interface (in black) and PS/PP interface (in white); a) and b) PS/PP/HDPE 10/45/45 and c) and d) PS/PP/HDPE/SEB1 10/45/45/(1% on PS content) after 30 min of quiescent annealing time.

copolymer. In this work, the minimum value of interfacial tension obtained is 3.0 ± 0.4 mN/m with 1% SEB3. Although this variation appears to be small, it has a clear and significant effect on the resulting microstructure.

In order to understand the discrepancy between these techniques more fully, the PS/HDPE interfacial tension modified with the SEB3 was also measured using the breaking thread method. HDPE was initially blended with 20% SEB3 (which represents the limit for the material transparency). The resulting average interfacial tension for three samples tested gives a value of 0.5 ± 0.2 mN/m, which is significantly below the value of 3.0 ± 0.4 mN/m for a saturated interface found by the Neumann triangle method above.

One possible explanation for the higher interfacial tension values observed by the Neumann method, as mentioned above, is that both $\gamma_{PS/PP}$ and $\gamma_{PP/HDPE}$ could be modified such that Γ_{PP} remains constant. That is to say that the SEB copolymer modifies the PS/PP and PP/HDPE interfaces as well as that between PS and HDPE. This would ultimately lead to a smaller value of $\gamma_{PS/HDPE}$. However, this seems unlikely, since SEB normally has a very low affinity for the PP/HDPE interface. Furthermore the experimental evidence in this work, related to the migration of the droplet to the PE side of the interface with increasing SEB concentration, strongly indicates that the SEB copolymer is selective for the PE/PS interface.

The differences between the interfacial tension values obtained by the breaking thread and the Neumann approaches also do not appear to be due to the poor migration of the copolymer to the interface in the partially wet systems. It has already been discussed in the previous section that there is very strong evidence in this study to support the notion that the PS/HDPE interface is saturated by SEB copolymer. In the next section, a potential explanation for this higher interfacial tension, based on the interfacial elasticity of a modified interface, will be examined.

3.4. Effect of the elasticity of the compatibilized interface

An elasticity effect arises when there is a variation of the interfacial tension as various kinds of interfacial deformations occur, such as an increase or a decrease of the area [34,46] (Fig. 10). For the case of a PS droplet with a modified PS/HDPE interface, the initial modification of the interface results in a decrease of the PS/HDPE interfacial tension and a subsequent relocation of the droplet towards the HDPE side (Fig. 10a–c).

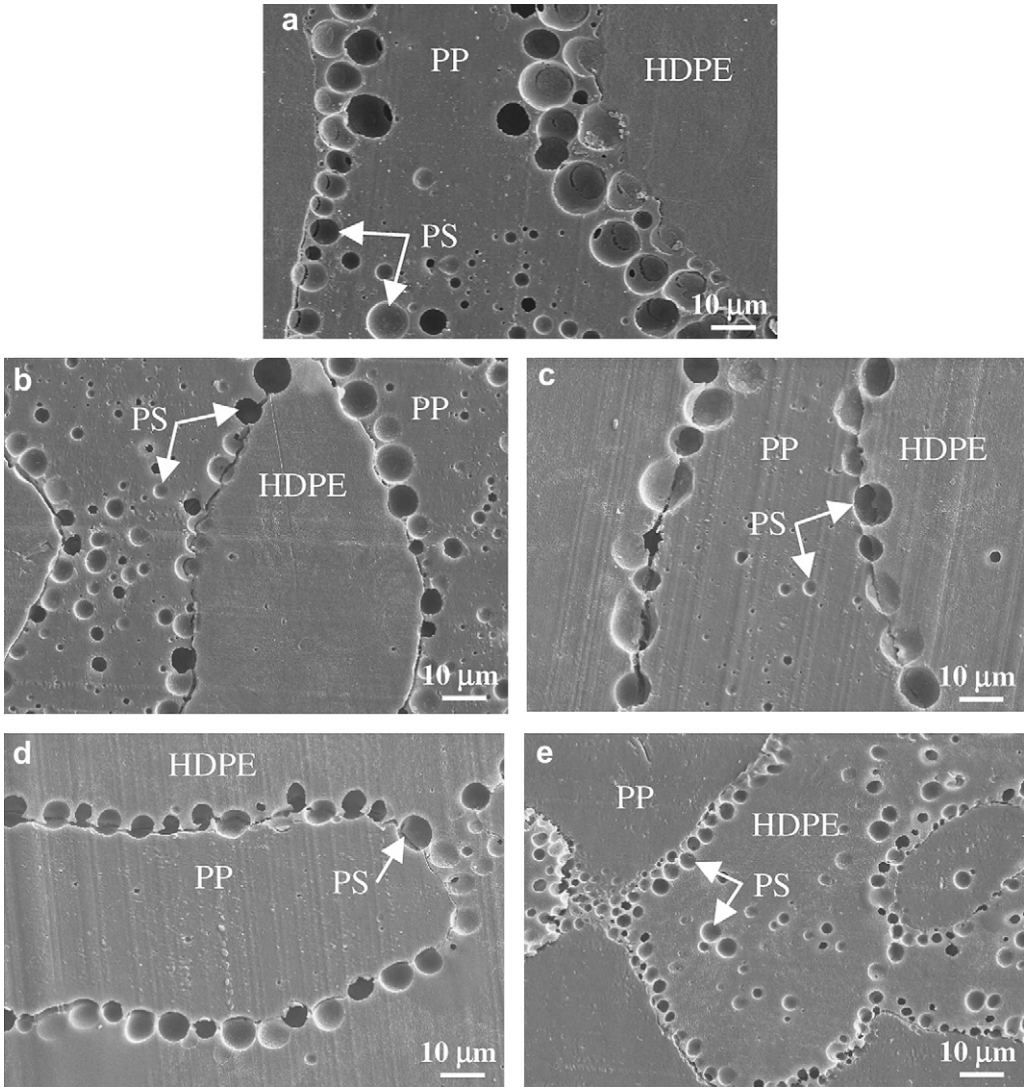

Fig. 7. SEM micrographs of PS/PP/HDPE 10/45/45 blends after 30 min of quiescent annealing showing the migration of the PS droplets towards the HDPE phase as the SEB3 concentration increases. a) 0% SEB3; b) 0.1% SEB3; c) 0.5% SEB3; d) 1% SEB3 and e) 2% SEB3.

However, as the droplet moves towards the HDPE, the PS/HDPE interfacial area increases (Fig. 10b and c), resulting in a simultaneous dilution of the copolymer at the interface and in an increase of the interfacial tension. The equilibrium position of the droplet at the interface results from two competing forces: one is due to the interfacial tension that drives the PS into the HDPE phase, and another which opposes that movement, due to the copolymer dilution, which is related to the interfacial elasticity. This effect would not be observed for an uncompatibilized interface since a variation of the interfacial area in that case does not induce a modification of the interfacial tension. Note that this interfacial elasticity is not to be confounded with material elasticity, which is an entropic effect that arises during dynamic melt processing due to the deformation of homopolymer chains from their equilibrium conformation.

This interfacial elasticity effect in compatibilized systems has to be taken into account in the thermodynamic analysis leading to the equilibrium conditions for capillary systems displaying a line of 3-phase contact. Li and Neumann [34,46] have demonstrated that it leads to a modified Neumann equation (decomposed here following two orthonormal axes):

$$\left(\gamma_{AC}^{\mathrm{mod}}+r_{AC}\left(\frac{\partial\gamma_{AC}^{\mathrm{mod}}}{\partial r_{AC}}\right)+\frac{\alpha}{2}\left(\frac{\partial\gamma_{AC}^{\mathrm{mod}}}{\partial\alpha}\right)\right)\cos\alpha+\gamma_{AB}\cos\beta=\gamma_{BC} \quad (6a)$$

$$\left(\gamma_{AC}^{\mathrm{mod}}+r_{AC}\left(\frac{\partial\gamma_{AC}^{\mathrm{mod}}}{\partial r_{AC}}\right)+\frac{\alpha}{2}\left(\frac{\partial\gamma_{AC}^{\mathrm{mod}}}{\partial\alpha}\right)\right)\sin\alpha=\gamma_{AB}\sin\beta \quad (6b)$$

The additional term $r_{AC}(\partial\gamma_{AC}^{\mathrm{mod}}/\partial r_{AC})$ accounts for the elasticity effect when the curvature r_{AC} varies while the angle α remains constant (Fig. 10d). The second additional term $(\alpha/2)(\partial\gamma_{AC}^{\mathrm{mod}}/\partial\alpha)$ accounts for the elasticity effect when the angle α varies while r_{AC} remains constant (Fig. 10e). It is clear that both of these contributions arise when the interfacial tension is dependant of the interfacial area, such as when it is modified with a copolymer.

Looking at these equations, the value of an apparent modified interfacial tension $\gamma_{AC}^{\mathrm{mod,\ apparent}}$ obtained with the Neumann triangle relation is in fact a combination of the real modified interfacial tension $\gamma_{AC}^{\mathrm{mod}}$ and the interfacial elasticity terms. Since the interfacial tension generally increases when the areal density in copolymer decreases, $r_{AC}(\partial\gamma_{AC}^{\mathrm{mod}}/\partial r_{AC})$ and $(\alpha/2)(\partial\gamma_{AC}^{\mathrm{mod}}/\partial\alpha)$ should be positive. Adding these contributions to the real modified

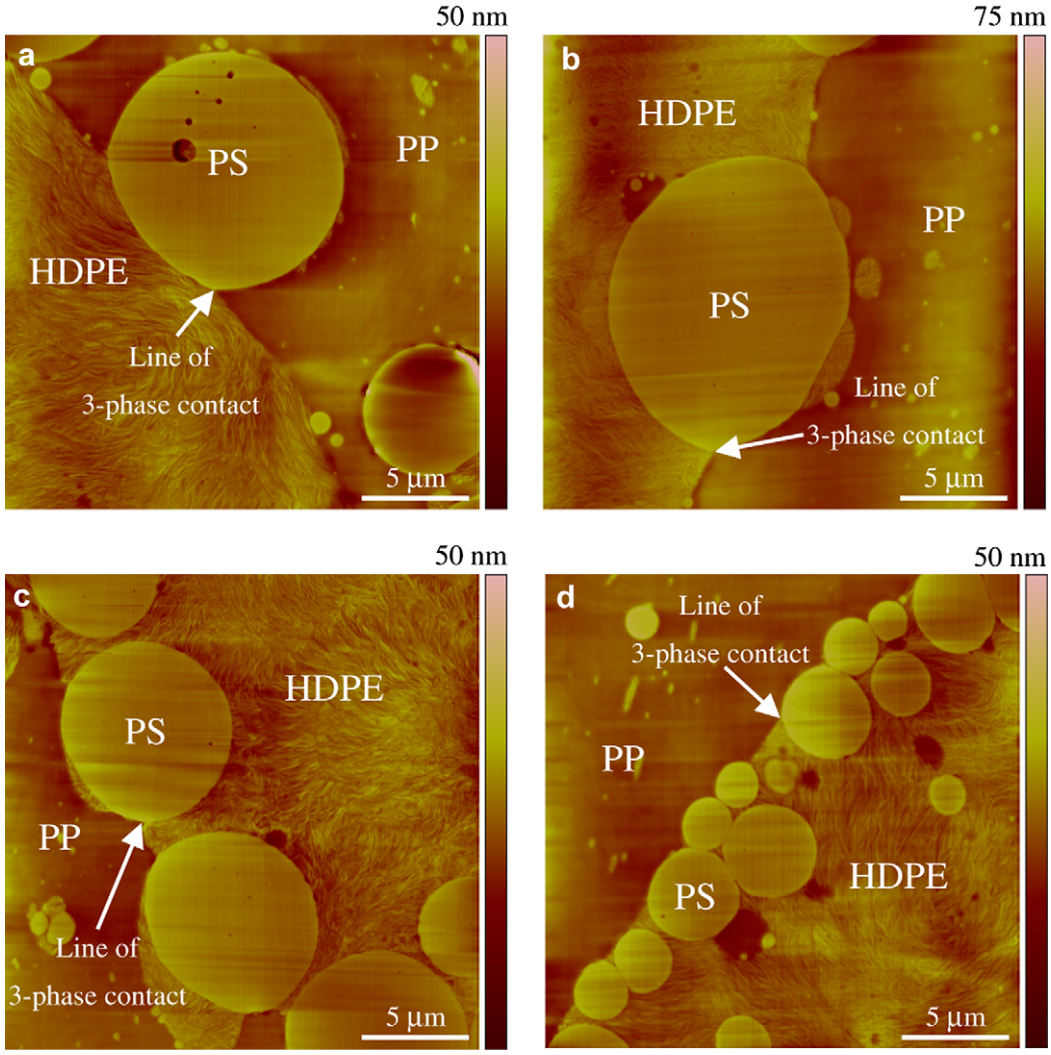

Fig. 8. FIB-AFM micrographs of PS/PP/HDPE 10/45/45 blends after 30 min of quiescent annealing used for the Neumann triangle analysis, showing the gradual migration of the PS droplets towards the HDPE phase as the concentration in SEB3 increases. a) 0.1% SEB3; b) 0.5% SEB3; c) 1% SEB3 and d) 2% SEB3.

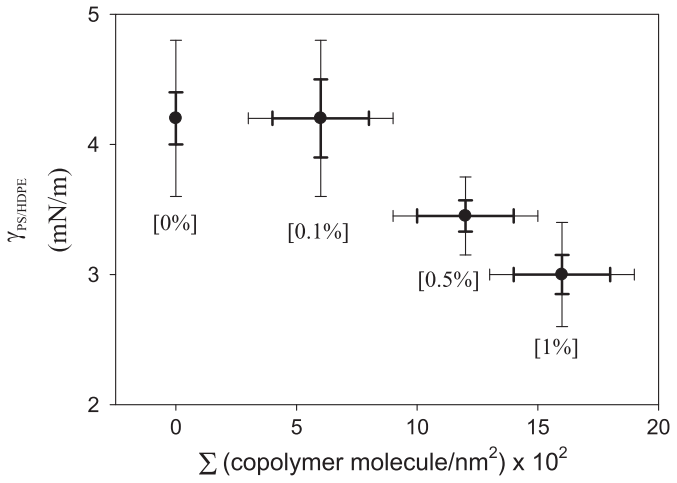

Fig. 9. Value of the modified PS/HDPE interfacial tension as a function of the SEB3 copolymer apparent areal density at the interface. The larger error bars correspond to the standard deviation σ and the smaller ones to the 95% confidence interval CI. The copolymer concentration, based on the PS phase volume, is shown in brackets.

interfacial tension γ_{AC}^{mod} results in an apparent modified tension $\gamma_{AC}^{mod,\ apparent}$ that overestimates the value of the true modified interfacial tension:

$$\gamma_{AC}^{mod,apparent} - \gamma_{AC}^{mod} = r_{AC}\left(\frac{\partial\gamma_{AC}^{mod}}{\partial r_{AC}}\right) + \frac{\alpha}{2}\left(\frac{\partial\gamma_{AC}^{mod}}{\partial\alpha}\right) > 0 \qquad (7)$$

Interfacial elasticity could then potentially explain why the modified interfacial tension values obtained by the Neumann triangle method are surprisingly high. What is in fact being measured is a combination of competing forces between the interfacial tension and interfacial elasticity [46].

Li and Neumann [34,46] also demonstrated that interfacial elasticity leads to a modified form of the classical Laplace equation. This effect should then be considered (or at least investigated) when using methods such as the sessile drop or the pendant drop to measure modified interfacial tensions. The analysis of interfacial elasticity is more complicated for the breaking thread technique since the geometry is significantly different and because it is a dynamic method.

As the experimental work of this paper has shown, interfacial elasticity can make morphology transitions more difficult since it

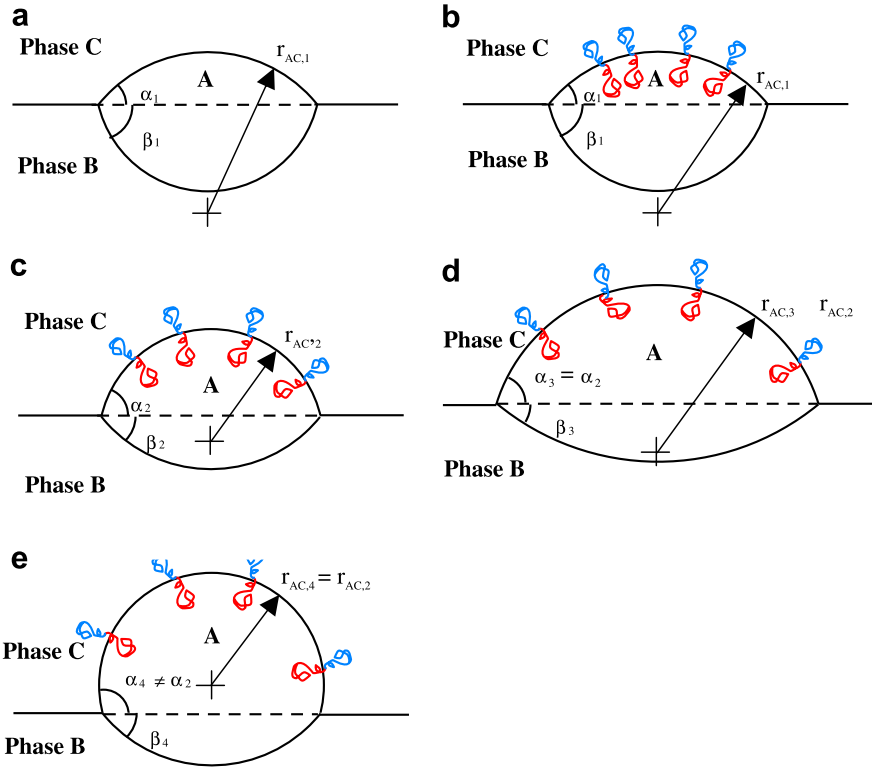

Fig. 10. Effect of interfacial elasticity on the apparent modified interfacial tension for a compatibilized ternary system displaying a line of 3-phase contact. a) Initial system without copolymer. Droplet is principally in Phase B; b) System after compatibilization of the AC interface. Droplet is still principally in Phase B.; c) re-localization of the droplet towards Phase C and dilution of the copolymer at the AC interface, interfacial elasticity present; d) variation of γ_{AB} when r_{AB} is increased while keeping the angle α constant and e) variation of γ_{AB} when α is increased while r_{AB} is kept constant.

opposes the effect of interfacial tension. Furthermore, while the resulting type of morphology for an uncompatibilized ternary blend does not depend on the geometrical parameters of the phases, it could be different for compatibilized systems since interfacial elasticity depends on the radius r and angle α (Equations 6a and b). It could then be possible to modify the system's wetting behaviour [5,6,31] not only by controlling the architecture and the amount of the added compatibilizer, but also by the geometry and size of the phases. This could have an important impact on morphology control in multicomponent systems. In a future paper from our laboratory, it will be demonstrated how the control of these partial/complete wetting morphologies, by selective interfacial modification in a quaternary immiscible polymer blend, can be a route towards the fabrication of ultraporous poly(L-lactide) scaffolds with complex microstructures. Finally, one of the main challenges in future experimental studies will be to separate the effects of the real modified interfacial tension and of the interfacial elasticity.

4. Conclusion

This article reports on the measurement of modified PS/HDPE interfacial tensions in a partially wet HDPE/PP/PS system using an *in situ* Neumann triangle method combined with a focused ion beam-atomic force microscopy sample preparation/analysis technique. The effect of five different SEB, SB and SEBS interfacial modifiers on the position of the PS droplet at the PE/PP interface was investigated. Except for the SEBS, which shows no effect at all, the addition of 1% copolymer (based on the PS content) results in a significant morphology transition, with the PS droplets exclusively relocating at the PP/HDPE interface. In addition, it is shown that the position of the PS droplet at the interface provides an indication of the ability of the particular copolymer to reduce interfacial tension. The PS droplets modified with the symmetrical diblock copolymer of 67 K molecular weight (SEB3) completely segregates to the PE/PP interface. This copolymer was most effective at locating preferentially at the PS/PE interface.

Using the Neumann triangle method, it is shown that using 1% of the symmetric SEB3 copolymer results in a slightly lower interfacial tension (3.0 ± 0.4 mN/m, 0.16 ± 0.03 copolymer molecule/nm^2) compared to an asymmetric one (3.3 ± 0.4 mN/m, 0.20 ± 0.07 copolymer molecule/nm^2). The areal density of copolymer at the interface was also estimated and the values show that the copolymer concentrates at the interface. The calculated values of areal density correlate well with other values from the literature for saturated interfaces. The interfacial tension for the SEB3 copolymer was measured as a function of the apparent areal density in copolymer and the results show a gradual decrease of the PS/HDPE interfacial tension as the content in symmetric SEB3 increases from 0% to 0.1%, 0.5% and 1%. However, in all cases, the modified interfacial tension values were significantly superior by about 2.5 mN/m compared to measurements performed with the breaking thread method (0.5 ± 0.2 mN/m). Experimental observations tend to show that the migration of the SEB3 to the PS/HDPE interface is highly effective and these unexpectedly high values of the modified interfacial tensions are attributed to an interfacial elasticity effect. In fact two competing forces exist: one purely interfacial tension driven force tending to locate the PS into the PE phase and another which opposes that movement, due to the copolymer dilution,

which is the interfacial elasticity. Interfacial elasticity is a phenomenon that could potentially play an important role not only in interfacial tension measurements, but also in such basic phenomena such as deformation/disintegration mechanisms in polymer blending and in morphology development.

Acknowledgments

The authors gratefully acknowledge the financial support received from the Natural Sciences and Engineering Research Council of Canada (NSERC). N. Virgilio would like to thank the Fonds Québécois de la Recherche sur la Nature et les Technologies (FQRNT) for a scholarship and Dr. Pierre Sarazin for fruitful discussions.

References

[1] Horiuchi S, Matchariyakul N, Yase K, Kitano T. Macromolecules 1997;30:3664–70.
[2] Guo HF, Packirisamy S, Gvozdic NV, Meier DJ. Polymer 1997;38:785–94.
[3] Guo HF, Gvozdic NV, Meier DJ. Polymer 1997;38:4915–23.
[4] Omonov TS, Harrats C, Groeninckx G. Polymer 2005;46:12322–36.
[5] Virgilio N, Aurèle C-M, Favis BD. Macromolecules 2009;42:3405–16.
[6] Virgilio N, Desjardins P, L'Espérance G, Favis BD. Macromolecules 2009;42:7518–29.
[7] Fayt R, Jérôme R, Teyssié P. Makromol Chem 1986;187:837–52.
[8] Matos M, Favis BD, Lomellini P. Polymer 1995;36:3899–907.
[9] Cigana P, Favis BD, Jérôme R. J Polym Sci B: Polym Phys 1996;34:1691–700.
[10] Cigana P, Favis BD. Polymer 1998;39:3373–8.
[11] Polizu S, Favis BD, Vu-Khanh T. Macromolecules 1999;32:3448–56.
[12] Li J, Favis BD. Polymer 2002;43:4935–45.
[13] Fayt R, Jérôme R, Teyssié P. J Polym Sci: Polym Lett 1986;24:25–8.
[14] Macosko CW, Guégan P, Khandpur A, Nakayama A, Maréchal P, Inoue T. Macromolecules 1996;29:5590–8.
[15] Adedeji A, Lyu S, Macosko CW. Macromolecules 2001;34:8663–8.
[16] Chang K, Macosko CW, Morse DC. Macromolecules 2007;40:3819–30.
[17] Retsos H, Margiolaki I, Messaritaki A, Anastasiadis SH. Macromolecules 2001;34:5295–305.
[18] Lepers J-C, Favis BD. AIChE J 1999;45:887–95.
[19] Mekhilef N, Favis BD, Carreau PJ. J Polym Sci B: Polym Phys 1997;35:293–308.
[20] Hu W, Koberstein JT, Lingelser JP, Gallot Y. Macromolecules 1995;28:5209–14.
[21] Elemans PHM, Janssen JMH, Meijer HEH. J Rheol 1990;34:1311–25.
[22] Anastasiadis SH, Gancarz I, Koberstein JT. Macromolecules 1989;22:1449–53.
[23] Van Hemelrijck E, Van Puyvelde P, Macosko CW, Moldenaers P. J Rheol 2005;49:783–98.
[24] Van Hemelrijck E, Van Puyvelde P, Velankar S, Macosko CW, Moldenaers P. J Rheol 2004;48:143–58.
[25] Bousmina M. Rheol Acta 1999;38:73–83.
[26] Jacobs U, Fahrlander M, Winterhalter J, Friedrich C. J Rheol 1999;43:1495–509.
[27] Riemann RE, Cantow HJ, Friedrich C. Macromolecules 1997;30:5476–84.
[28] Riemann RE, Cantow HJ, Friedrich C. Polym Bull 1996;36:637–43.
[29] Palierne JF. Rheol Acta 1990;29:204–14. Erratum 1991;30:497-497.
[30] Rowlinson JS, Widom B. Molecular theory of capillarity. Oxford: Oxford University Press; 1982.
[31] Torza S, Mason SG. J Coll Int Sci 1970;33:67–83.
[32] Chen P, Gaydos J, Neumann AW. Langmuir 1996;12:5956–62.
[33] Shadnam M, Amirfazli A. Langmuir 2003;19:4658–65.
[34] Li D, Neumann AW. Adv Coll Int Sci 1994;49:147–195.
[35] Hyun DC, Jeong U, Ryu DY. J Polym Sci B: Polym Phys 2007;45:2729–38.
[36] Kim JK, Jeong W-Y, Son J-M, Jeon HK. Macromolecules 2000;33:9161–5.
[37] Zhang X, Kim JK. Macromol Rapid Comm 1998;19:499–504.
[38] Debolt MA, Robertson RE. Polym Eng Sci 2006;46:385–96.
[39] De Freitas CA, Valera TS, De Souza AMC, Demarquette NR. Macromol Symp 2007;247:260–70.
[40] Virgilio N, Desjardins P, Pépin M-F, L'Espérance G, Favis BD. Macromolecules 2005;38:2368–75.
[41] Tomotika S. Proc Roy Soc London Ser A 1934;A150:322–37.
[42] Utracki LA, Shi ZH. Polym Eng Sci 1992;32:1824–33.
[43] Leibler L. Makromol. Chem Macromol Symp 1988;16:1–17.
[44] Leibler L. Physica A 1991;172:258–68.
[45] Hudson SD, Jamieson AM. In: Paul DR, Bucknall CB, editors. Polymer blends. Formulation. 1st ed., vol. 1. New York: Wiley-Interscience; 1999. Paul, D.R. and Bucknall, C.B.
[46] Li D, Neumann AW. Langmuir 1993;9:50–4.